

# Local $\alpha$ -removal strength in the mean-field approximation

Takashi Nakatsukasa<sup>1, 2, 3</sup> and Nobuo Hinohara<sup>1, 2, 4</sup>

<sup>1</sup>Center for Computational Sciences, University of Tsukuba, Tsukuba 305-8577, Japan

<sup>2</sup>Faculty of Pure and Applied Sciences, University of Tsukuba, Tsukuba 305-8571, Japan

<sup>3</sup>RIKEN Nishina Center, Wako 351-0198, Japan

<sup>4</sup>Facility for Rare Isotope Beams, Michigan State University, East Lansing, Michigan 48824, USA

(Dated: September 11, 2023)

**Background:** The  $\alpha$  cluster is a prominent feature, not only in light nuclei but also in heavy nuclei. To study the  $\alpha$ -particle formation in the mean-field calculation, the localization function has been extensively utilized. However, the localization function does not guarantee the proximity of four different nucleons which is required by the  $\alpha$ -particle formation. A simple indicator of the proximity is desired. Recently, experimental measurement of the quasifree  $\alpha$ -knockout reaction for Sn isotopes reveals the cross sections with a monotonic decrease with increasing neutron number. [Science **371**, 260 (2021)]. This is interpreted as evidence of the surface  $\alpha$  formation.

**Purpose:** We propose a simple and comprehensible quantity to assess the proximity of four nucleons with different spins and isospins. Using this, we examine the recent measurement of  $\alpha$ -knockout cross sections in Sn isotopes.

**Methods:** The local  $\alpha$ -removal strength is proposed to quantify the possibility to form an  $\alpha$  particle at a specific location inside the nucleus. In addition, it provides the strength of ground and excited states in the residual nuclei after the removal of the  $\alpha$  particle. To make the calculation feasible, we introduce several approximations, such as point- $\alpha$ , mean-field, and no rearrangement approximations. We use the Hartree-Fock-plus-BCS method for the mean-field calculation for Sn isotopes. We also propose another measure, the local  $\alpha$  probability, which should provide a better correlation with the  $\alpha$ -knockout cross sections.

**Results:** The calculation of the local  $\alpha$ -removal strength is extremely easy in the mean-field model with no rearrangement. For even-even Sn isotopes, the local  $\alpha$ -removal strengths to the ground state of residual nuclei are almost universal in the nuclear surface region. In contrast, the local  $\alpha$  probability produces strong neutron number dependence consistent with the experiment.

**Conclusions:** The local  $\alpha$ -removal strength and the local  $\alpha$  probability are easily calculable in the mean-field models. Recent experimental data for Sn isotopes may be explained by a simple model without explicit consideration of  $\alpha$  correlation.

## I. INTRODUCTION

Clustering is an intriguing phenomenon in the nuclear structure. Correlations between nucleons result in the formation of subunits (clusters) inside the nucleus. The most typical cluster is the  $\alpha$  particle, which is present not only in light nuclei, but also observed in heavy nuclei as the  $\alpha$ -decay phenomena. In light nuclei, prominent clustering often takes place in excited states whose energy is close to the threshold of the corresponding cluster decomposition [1].

The microscopic theories of the clustering phenomena have a long history [1–5]. In fact, Gamow’s theory of the  $\alpha$  decay [6, 7] was published even before the discovery of the neutron [8]. Most theoretical studies of the cluster structure in the past have been performed with an assumption that a certain cluster structure exists in the nucleus. It is common to construct the cluster wave functions in terms of the Gaussian wave packets [9]. For instance, the antisymmetric molecular dynamics (AMD) [10] and the fermionic molecular dynamics (FMD) [11] were extensively utilized in studies of the nuclear cluster phenomena and heavy-ion reactions. In the AMD and FMD, the cluster structure is not assumed *a priori*, although the Gaussian wave packet is assumed for a single-particle state [12–14]. The configuration mixing,

which is often treated with the projection and the generator coordinate method [15, 16], plays an important role in the studies of clustering in relatively light nuclei. In the AMD and FMD, since each Gaussian has parameters corresponding to the position of its center and the magnitude of its width, the clustering can be identified by close location of centers of many Gaussian wave packets.

In contrast, the mean-field (energy density functional) theory can provide the optimal single-particle wave functions to minimize the total energy of a Slater determinant. One of the advantageous features of the theory is the capability of describing almost all the nuclei in the nuclear chart using a single energy density functional which is a functional of normal and pair densities. Another advantage can be the treatment of the pairing correlations, which become indispensable especially for heavy nuclei with open-shell configurations. The obtained (generalized) single-particle states are, in most cases, spread over the entire nucleus, not confined in a localized region inside the nucleus. Therefore, in the mean-field theory, it is not straightforward to find nucleons’ gathering in terms of the single-particle wave functions. In relatively light nuclei, prominent cluster structure could be observed by the nucleon density profile [17–21]. In particular, the clustering phenomena have been extensively studied with relativistic energy density functionals [22].

The cluster structure in the relativistic energy density functionals, such as DD-ME2, is more visible than in the nonrelativistic functionals, producing spatially localized subunits inside the nucleus [23]. However, the identification of the cluster structure has some ambiguity and relies on one's intuition.

There exist some methods aiming to identify and quantify the clustering effect in the mean-field states. In case one can intuitively build a model cluster wave function, its overlap with the mean-field state gives a possible measure of the clustering [19]. Recently, another method, which does not require a model wave function, has been proposed to visualize possible cluster correlations using the mean-field wave functions [24]. However, the application of the method seemingly become more and more difficult as the nucleon number increases.

The localization function, introduced into nuclear physics by Reinhard and collaborators [25], is a possible measure of  $\alpha$ -particle formation. Similar functions were introduced in molecular physics to investigate the shell structure and the chemical bonding [26]. Since it only needs one-body densities, such as kinetic and current densities, the calculation requires negligible computational cost. In addition, it is given as a function of the spatial coordinates. Thus, one can identify the location of the  $\alpha$  particles. Because of these advantageous properties, the localization function has been adopted in a number of studies for the cluster correlations within the mean-field theory [27–32]. However, it should be noted that the localization function does not examine whether the four nucleons exist next to each other. It tells us information on the conditional pair density for particles of the same kind,  $P_{q\sigma}(\mathbf{r}, \mathbf{r}')$  where  $q = n, p$  and  $\sigma = \pm 1/2$ . Reference [25] clearly states that the localization function is just the first step to identifying the  $\alpha$  cluster. The  $\alpha$  cluster requires the four nucleons to gather in a localized region inside the nucleus, which cannot be checked by the localization function. Properties of the localization function were studied in Ref. [33], concluding that it is not sensitive to the compactness of the  $\alpha$  particle. Therefore, the purpose of the present paper is to propose the next step, “local  $\alpha$ -removal strength,” as a measure of *four localized nucleons* that can be easily estimated in the mean-field theory.

Experimentally, the  $\alpha$  correlations in nuclei can be investigated by quasifree  $\alpha$ -knockout reactions [34, 35]. A recent experiment on the  $\alpha$ -knockout reactions in Sn isotopes by Tanaka and collaborators [36] reveals that the cross section monotonically decreases as the neutron number increases. They interpret this trend as a tight interplay between the  $\alpha$  formation and the neutron skin [37]. The distorted-wave impulse-approximation study shows that the reaction takes place in a peripheral region and probes the  $\alpha$  particles in the nuclear surface [38]. Another purpose of the present paper is to examine consistency between the calculated local  $\alpha$ -removal strength and the result of Ref. [36].

The paper is organized as follows: We propose a feasi-

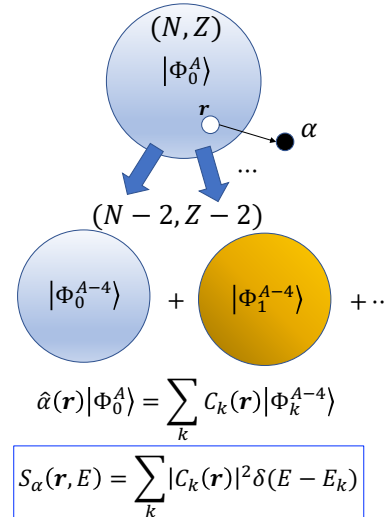


FIG. 1. Schematic illustration of the local  $\alpha$ -removal strength  $S_\alpha(\mathbf{r}, E)$ . Removing the  $\alpha$  particle located at a position  $\mathbf{r}$  from the nucleus  $(N, Z)$  results in many energy eigenstates of the residual nucleus  $(N - 2, Z - 2)$ , with  $C_k(\mathbf{r}) = \langle \Phi_k^{A-4} | \hat{\alpha}(\mathbf{r}) | \Phi_0^A \rangle$ . See Eq. (3).

ble measure of four-particle localization, local  $\alpha$ -removal strength, in Sec. II. In Sec. III, the local  $\alpha$ -removal strength is applied to Sn and other isotopes. The calculation is compared with the measurement of the  $\alpha$ -knockout reaction. Concluding remarks are given in Sec. IV.

## II. LOCAL $\alpha$ -REMOVAL STRENGTH

### A. Definition

Let us assume a single Slater-determinant description for the  $\alpha$  particle and that the orbital part of the single-particle wave functions are all the same and given by  $\phi_\alpha(\mathbf{r})$ , where the center of mass of the  $\alpha$  particle is located at the origin. Then, the  $\alpha$ -particle annihilation operator  $\hat{\alpha}(\mathbf{R})$  at the position  $\mathbf{R}$  is given by

$$\hat{\alpha}(\mathbf{R}) \equiv \int d\mathbf{r}_1 d\mathbf{r}_2 d\mathbf{r}_3 d\mathbf{r}_4 \phi_\alpha^*(\mathbf{r}_{1\mathbf{R}}) \phi_\alpha^*(\mathbf{r}_{2\mathbf{R}}) \phi_\alpha^*(\mathbf{r}_{3\mathbf{R}}) \phi_\alpha^*(\mathbf{r}_{4\mathbf{R}}) \times \hat{\psi}_\uparrow^{(n)}(\mathbf{r}_1) \hat{\psi}_\downarrow^{(n)}(\mathbf{r}_2) \hat{\psi}_\uparrow^{(p)}(\mathbf{r}_3) \hat{\psi}_\downarrow^{(p)}(\mathbf{r}_4) \quad (1)$$

where  $\mathbf{r}_{i\mathbf{R}} = \mathbf{r}_i - \mathbf{R}$  ( $i = 1, \dots, 4$ ) and  $\hat{\psi}_\sigma^{(q)}(\mathbf{r})$  indicates the field operator for the particle of the isospin  $q = n, p$  and the spin  $\sigma = \uparrow, \downarrow$ . The wave function  $\phi_\alpha(\mathbf{r})$  is a well-localized function, normally assumed to be a Gaussian in the cluster model.

To investigate the  $\alpha$  particle in the nucleus, we propose “local  $\alpha$ -removal strength” defined as

$$S_\alpha(\mathbf{r}, E) \equiv \langle \Phi_0^A | \hat{\alpha}^\dagger(\mathbf{r}) \delta(E - \hat{H}) \hat{\alpha}(\mathbf{r}) | \Phi_0^A \rangle, \quad (2)$$

where  $\hat{H}$  is the Hamiltonian, and  $|\Phi_0^A\rangle$  is the ground state of the nucleus ( $N, Z$ ).

The meaning of this quantity is clear if we insert the unity expanded in terms of the complete set for the nucleus ( $N - 2, Z - 2$ ),  $\{|\Phi_k^{A-4}\rangle\}$ :

$$S_\alpha(\mathbf{r}, E) = \sum_{k=0}^{\infty} |\langle \Phi_k^{A-4} | \hat{\alpha}(\mathbf{r}) | \Phi_0^A \rangle|^2 \delta(E - E_k^{A-4}), \quad (3)$$

where  $\hat{H}|\Phi_k^{A-4}\rangle = E_k^{A-4}|\Phi_k^{A-4}\rangle$ . Thus, the quantity

$$\begin{aligned} S_\alpha(\mathbf{r})_{E, \Delta E} &= \int_{E-\Delta E/2}^{E+\Delta E/2} S_\alpha(\mathbf{r}, E') dE' \\ &= \sum_k^{\Delta E} |\langle \Phi_k^{A-4} | \hat{\alpha}(\mathbf{r}) | \Phi_0^A \rangle|^2. \end{aligned} \quad (4)$$

provides the strength of the transition to states in the energy range  $(E - \Delta E/2, E + \Delta E/2)$  of the residual nucleus, when the  $\alpha$  particle is removed at the position  $\mathbf{r}$  in the nucleus ( $N, Z$ ). See also Fig. 1.

It is convenient to define the variable  $E$  with respect to the ground-state energy  $E_0^{A-4}$ , namely, the excitation energy  $E' = E - E_0^{A-4}$ . Hereafter, we denote  $E'$  as  $E$  for simplicity. Appropriate smearing of the  $\delta$  function  $\delta(E - E_k^{A-4})$  may be useful for visualizing the strength as a function of  $E$ . The local  $\alpha$ -removal strength  $S_\alpha(\mathbf{r}, E)$  may provide transition strength to states at the excitation energy  $E$ , when the  $\alpha$  particle is removed at the position  $\mathbf{r}$ .

## B. Approximations

The calculation of Eq. (2) demands a large computational cost in general. We introduce here some approximations to make the computation feasible.

### 1. Point $\alpha$ approximation

First, in order to avoid the multiple integrations in Eq. (1), we approximate the wave function  $\phi_\alpha(\mathbf{r})$  by the  $\delta$  function  $\delta(\mathbf{r} - \mathbf{R})$ . Thus, in this paper, we use

$$\hat{\alpha}(\mathbf{r}) = \hat{\psi}_\uparrow^{(n)}(\mathbf{r}) \hat{\psi}_\downarrow^{(n)}(\mathbf{r}) \hat{\psi}_\uparrow^{(p)}(\mathbf{r}) \hat{\psi}_\downarrow^{(p)}(\mathbf{r}). \quad (5)$$

This approximation significantly reduces the computational cost. Without the point  $\alpha$  approximation, the numerical cost of the multiple integrals with respect to the four coordinates is extremely large. Since the Gaussian wave function for the  $\alpha$  particle is compact, the point  $\alpha$  approximation is able to provide a useful signal of the localized four nucleons. Further approximations in the following sections lead to products of pair densities  $\langle \hat{\psi}_\uparrow^{(q)}(\mathbf{r}_1) \hat{\psi}_\downarrow^{(q)}(\mathbf{r}_2) \rangle$ . Without the point  $\alpha$  approximation, we need nonlocal pair densities with  $\mathbf{r}_1 \neq \mathbf{r}_2$ , whose behavior is not well controlled in currently available pairing energy density functionals.

## 2. Mean-field approximation

Next, we adopt the mean-field ground state for  $|\Phi_0^A\rangle$ , and the Hamiltonian  $\hat{H}$  is approximated in the mean-field level.  $\hat{H}$  is truncated up to the second order in terms of the quasiparticle (qp) operators defined with respect to the ground state of the residual nucleus ( $N - 2, Z - 2$ ):

$$\hat{H} = \sum_{q=n, p} \sum_{i>0} E_i^{(q)} \hat{a}_i^{(q)\dagger} \hat{a}_i^{(q)} + \dots, \quad (6)$$

where the ground-state energy of the nucleus ( $N - 2, Z - 2$ ),  $E_0^{A-4} = \langle \Phi_0^{A-4} | \hat{H} | \Phi_0^{A-4} \rangle$ , is subtracted.  $\hat{a}_i^{(q)}$  and  $E_i^{(q)}$  are the qp annihilation operators and corresponding qp energies. The subscript  $i > 0$  means the summation with respect to the qp states with positive qp energies  $E_i^{(q)} > 0$ . In Eq. (3), the excited states ( $k > 0$ ) are given by an even number of qp excitations. Thus, the index  $k$  stands for 2qp, 4qp,  $\dots$  and the excitation energies  $E_k^{A-4}$  ( $k > 0$ ) in Eq. (3) are given as

$$E_{ij,0}^{A-4} = E_i^{(n)} + E_j^{(n)}, \quad (7)$$

$$E_{0,ij}^{A-4} = E_i^{(p)} + E_j^{(p)}, \quad (8)$$

$$E_{ij,i'j'}^{A-4} = E_i^{(n)} + E_j^{(n)} + E_{i'}^{(p)} + E_{j'}^{(p)}, \quad (9)$$

and so on.

With the mean-field construction of the states,  $|\Phi_0^A\rangle$  and  $|\Phi_0^{A-4}\rangle$ , one can calculate the transition matrix elements  $\langle \Phi_k^{A-4} | \hat{\alpha}(\mathbf{r}) | \Phi_0^A \rangle$  in Eq. (3) as follows. Except for the cases under the presence of proton-neutron ( $pn$ ) pairing [39–41] and/or  $pn$  mixing [42, 43], the states are normally described by product wave functions of protons and neutrons,  $|\Phi^A\rangle = |\Phi^N\rangle \otimes |\Phi^Z\rangle$ . Therefore, the transition matrix elements can be also written in the product form,  $\langle \Phi_k^{N-2} | \hat{\psi}_\uparrow^{(n)}(\mathbf{r}) \hat{\psi}_\downarrow^{(n)}(\mathbf{r}) | \Phi_0^N \rangle \langle \Phi_{k'}^{Z-2} | \hat{\psi}_\uparrow^{(p)}(\mathbf{r}) \hat{\psi}_\downarrow^{(p)}(\mathbf{r}) | \Phi_0^Z \rangle$ , where  $k$  ( $k'$ ) stands for 0qp, 2qp,  $\dots$  indices for neutrons (protons). Thus,

$$S_\alpha(\mathbf{r}, E) = \sum_{k \geq 0} \sum_{k' \geq 0} F_k^{(n)}(\mathbf{r}) F_{k'}^{(p)}(\mathbf{r}) \delta(E - E_{kk'}^{A-4}), \quad (10)$$

where  $E_{kk'}^{A-4}$  are given by Eqs. (7)–(9), and

$$F_k^{(q)}(\mathbf{r}) = \left| \langle \Phi_k^{N_q-2} | \hat{\psi}_\uparrow^{(q)}(\mathbf{r}) \hat{\psi}_\downarrow^{(q)}(\mathbf{r}) | \Phi_0^{N_q} \rangle \right|^2, \quad (11)$$

with  $N_q = N$  and  $Z$  for  $q = n$  and  $p$ , respectively.

## 3. Neglect of rearrangement

We introduce further approximation to neglect the rearrangement of the mean fields due to the removal of the  $\alpha$  particle. Hence, we assume that the mean fields in nuclei of mass number  $A$  and  $A - 4$  (before and after the removal of an  $\alpha$  particle) are identical. When the

neutrons (protons) are in a superfluid phase, we also neglect the change of the chemical potential, which leads to  $|\Phi_k^{N_q-2}\rangle \approx |\Phi_k^{N_q}\rangle$  with  $q = n$  ( $p$ ). With this approximation, the calculation of the residual states ( $|\Phi_k^{A-4}\rangle$ ) is no longer required. The mean-field Hamiltonian (6) is now replaced by that for the nucleus ( $N, Z$ ), in which all the quasiparticle states are defined with respect to the mean-field ground state of  $|\Phi_0^A\rangle$ .

Assuming the Bogoliubov transformation [44],

$$\hat{a}_i^\dagger = \sum_{\sigma} \int d\mathbf{r} \left\{ U_i(\mathbf{r}\sigma) \hat{\psi}_\sigma^\dagger(\mathbf{r}) + V_i(\mathbf{r}\sigma) \hat{\psi}_\sigma(\mathbf{r}) \right\} \quad (12)$$

$$\hat{\psi}_\sigma^\dagger(\mathbf{r}) = \sum_{i>0} \left\{ U_i^*(\mathbf{r}\sigma) \hat{a}_i^\dagger + V_i(\mathbf{r}\sigma) \hat{a}_i \right\}, \quad (13)$$

the matrix elements  $F_k^{(q)}(\mathbf{r})$  of Eq. (11) are given as

$$F_0(\mathbf{r}) = \left| \sum_{i>0} U_i(\mathbf{r}\uparrow) V_i^*(\mathbf{r}\downarrow) \right|^2 = |\kappa(\mathbf{r})|^2, \quad (14)$$

$$F_{ij}(\mathbf{r}) = \left| V_i^*(\mathbf{r}\uparrow) V_j^*(\mathbf{r}\downarrow) - V_j(\mathbf{r}\uparrow) V_i(\mathbf{r}\downarrow) \right|^2, \quad (15)$$

where the superscript ( $q$ ) is omitted for simplicity.  $F_0(\mathbf{r})$  is nothing but a square of the local pair density,  $|\kappa(\mathbf{r})|^2 \equiv |\langle \Phi_0^A | \hat{\psi}_\uparrow(\mathbf{r}) \hat{\psi}_\downarrow(\mathbf{r}) | \Phi_0^A \rangle|^2$ . It should be also noted that, with this approximation, only the 0qp and 2qp excitations of neutrons and protons contribute to the summation with respect to  $k$  and  $k'$  in Eq. (10).

For the transition to the ground state, which may be of most interest, the calculation is feasible with these approximations. Its relative values among different isotopes may be a useful indicator of the  $\alpha$ -particle knockout probability. However, we should keep in mind that this is based on the approximations adopted, and should be careful especially when we compare the values for nuclei in different mass regions.

#### 4. HF-plus-BCS approximation

Using the HF-plus-BCS (HF+BCS) approximation, the HFB wave functions are proportional to the HF single-particle states  $\{\phi_i(\mathbf{r}\sigma)\}$  as

$$\begin{aligned} U_i(\mathbf{r}\sigma) &= u_i \phi_i(\mathbf{r}\sigma), & V_i(\mathbf{r}\sigma) &= -v_i \phi_i^*(\mathbf{r}\sigma), \\ U_{\bar{i}}(\mathbf{r}\sigma) &= u_{\bar{i}} \phi_{\bar{i}}(\mathbf{r}\sigma), & V_{\bar{i}}(\mathbf{r}\sigma) &= v_{\bar{i}} \phi_{\bar{i}}^*(\mathbf{r}\sigma), \end{aligned} \quad (16)$$

where  $\phi_{\bar{i}}$  is the time-reversal partner of  $\phi_i$ . The BCS uv factors,  $(u_i, v_i)$ , are all real and determined by the HF single-particle energies [44]. This recasts Eqs.(14) and (15) into

$$F_0(\mathbf{r}) = |\kappa(\mathbf{r})|^2 = \left| \sum_i u_i v_i \phi_i(\mathbf{r}\uparrow) \phi_i(\mathbf{r}\downarrow) \right|^2 \quad (17)$$

$$F_{ij}(\mathbf{r}) = v_i^2 v_j^2 |\phi_i(\mathbf{r}\uparrow) \phi_j(\mathbf{r}\downarrow) - \phi_j(\mathbf{r}\uparrow) \phi_i(\mathbf{r}\downarrow)|^2. \quad (18)$$

The summation in Eq. (17) is taken over both  $i$  and  $\bar{i}$  with  $\phi_{\bar{i}} = -\phi_i$ ,  $u_{\bar{i}} = u_i$ , and  $v_{\bar{i}} = v_i$ .<sup>1</sup> Since the indices  $ij$  and  $ji$  correspond to the same 2qp excitation, the summation in Eq. (10) is performed with respect to different combinations of 2qp indices, namely with the restriction of  $i > j$ .

The pairing gap  $\Delta_q$  ( $q = n, p$ ) is related to the monopole pairing strength  $G$  as  $\Delta_q = \frac{1}{2}G \sum_i u_i v_i$  [44]. In this paper, we adopt the value of  $\Delta_q$  as the experimental odd-even mass difference.

#### 5. No pairing case

In case there is no pairing (normal phase) in the state  $|\Phi_0^{N_q}\rangle$ , Eq. (14) does not give a transition to the ground state because the pair density trivially vanishes. This is due to the wrong approximation of  $|\Phi_k^{N_q-2}\rangle \approx |\Phi_k^{N_q}\rangle$  for the normal phase. In this case,  $|\Phi_0^{N_q}\rangle$  is the Hartree-Fock (HF) ground-state wave function. Then, we explicitly remove two particles from the occupied orbitals in  $|\Phi_0^{N_q}\rangle$ , and identify it as  $|\Phi_k^{N_q-2}\rangle$  in Eq. (11). This leads to

$$F_{ij}(\mathbf{r}) = |\phi_i(\mathbf{r}\uparrow) \phi_j(\mathbf{r}\downarrow) - \phi_j(\mathbf{r}\uparrow) \phi_i(\mathbf{r}\downarrow)|^2, \quad (20)$$

where  $\phi_i$  and  $\phi_j$  are the single-particle wave functions for the occupied (hole) states. The expression is equal to Eq. (15) by identifying  $V_i^* = \phi_i$  ( $V_i^* = 0$ ) for hole (particle) states. Note that  $ij$  are the two-hole indices which include not only the excited states ( $k > 0$ ) but also the ground state ( $k = 0$ ) in  $|\Phi_k^{N_q-2}\rangle$ . For the ground state  $|\Phi_0^{N_q-2}\rangle$ , two particles  $ij$  are removed from the highest occupied orbitals (HOO).

The ground state of the residual nucleus ( $N-2, Z-2$ ) is unique when the ground state of the nucleus ( $N, Z$ ) is superfluid both in protons and neutrons. However, we should remark here that, for the normal state (no pairing), there may be multiple ground states with the present approximations. This is an undesired consequence of no rearrangement, and it occurs when the nucleus  $|\Phi_0^A\rangle$  is spherical, because the HOO with the angular momentum  $j$  should have a degeneracy of  $2j+1$ . To keep the feasibility in the computation, we simply sum up all the possible two-hole indices to produce  $F_0$  for nuclei in the normal phase.

$$F_0(\mathbf{r}) = \sum_{ij \in \text{HOO}} |\phi_i(\mathbf{r}\uparrow) \phi_j(\mathbf{r}\downarrow) - \phi_j(\mathbf{r}\uparrow) \phi_i(\mathbf{r}\downarrow)|^2. \quad (21)$$

<sup>1</sup> Explicitly denoting the time-reversal parts, Eq. (17) can be written as

$$F_0(\mathbf{r}) = \left| \sum_{i \gg 0} u_i v_i \{ \phi_{\bar{i}}(\mathbf{r}\uparrow) \phi_i(\mathbf{r}\downarrow) - \phi_i(\mathbf{r}\uparrow) \phi_{\bar{i}}(\mathbf{r}\downarrow) \} \right|^2. \quad (19)$$

Here,  $i \gg 0$  indicates the summation is not taken over  $\bar{i}$ . Note that it is different from  $i > 0$  in Eq. (6).

### C. Localization function

We will compare the local  $\alpha$ -removal strength with the localization function  $C_\sigma^{(q)}(\mathbf{r})$  in Sec. III. It may be useful to recapitulate the definition and the meaning of  $C_\sigma^{(q)}(\mathbf{r})$ , according to Ref. [25].

The conditional probability of finding a nucleon with spin  $\sigma$  and isospin  $q$  at  $\mathbf{r}'$  when another nucleon with the same spin and isospin exists at  $\mathbf{r}$  is given by

$$P_\sigma^{(q)}(\mathbf{r}, \mathbf{r}') = \rho_\sigma^{(q)}(\mathbf{r}') - \left| \rho_{\sigma\sigma}^{(q)}(\mathbf{r}, \mathbf{r}') \right|^2 / \rho_\sigma^{(q)}(\mathbf{r}), \quad (22)$$

where, in the mean-field calculations,

$$\rho_{\sigma\sigma'}(\mathbf{r}, \mathbf{r}') \equiv \sum_{i>0} V_i^*(\mathbf{r}\sigma) V_i(\mathbf{r}'\sigma'), \quad (23)$$

and  $\rho_\sigma(\mathbf{r}) = \rho_{\sigma\sigma}(\mathbf{r}, \mathbf{r})$ . Again, hereafter in this section, the superscript  $(q)$  is omitted for simplicity. Let us rewrite  $P_\sigma(\mathbf{r}, \mathbf{r}') = P_\sigma(\mathbf{R}, \mathbf{s})$  in terms of the average and the relative positions,  $\mathbf{R} = (\mathbf{r} + \mathbf{r}')/2$  and  $\mathbf{s} = \mathbf{r} - \mathbf{r}'$ , then, perform a spherical averaging over the angles of  $\mathbf{s}$ . Finally, we expand the  $P_\sigma(\mathbf{r}, s)$  with respect to  $s$  as

$$\begin{aligned} P_\sigma(\mathbf{r}, s) &\approx \frac{1}{3} \left( \tau_\sigma - \frac{1}{4} \frac{(\nabla \rho_\sigma)^2}{\rho_\sigma} - \frac{\mathbf{j}_\sigma^2}{\rho_\sigma} \right) s^2 \\ &\equiv \frac{1}{3} D_\sigma(\mathbf{r}) s^2 \end{aligned} \quad (24)$$

Then, the localization function  $C_\sigma(\mathbf{r})$  is defined as  $C_\sigma(\mathbf{r}) = [1 + \{D_\sigma(\mathbf{r})/\tau^{\text{TF}}(\mathbf{r})\}^2]^{-1}$ , where the Thomas-Fermi kinetic density  $\tau_\sigma^{\text{TF}}(\mathbf{r}) = 3(6\pi^2)^{2/3} \rho_\sigma^{5/3}$  is introduced to make  $C_\sigma(\mathbf{r})$  dimensionless.  $P_\sigma(\mathbf{r}, s) \rightarrow 0$  at  $s \rightarrow 0$  is guaranteed by the Pauli exclusion principle. The definition restricts the range of  $C_\sigma(\mathbf{r})$  as  $0 < C_\sigma(\mathbf{r}) \leq 1$ . It is apparent that the smaller the conditional probability  $P_\sigma(\mathbf{r}, s)$  is, the larger the localization function  $C_\sigma(\mathbf{r})$ . In other words,  $C_\sigma^{(q)}(\mathbf{r}) \approx 1$  indicates very little probability of finding two nearby nucleons with the same spin  $\sigma$  and isospin  $q$  around the position  $\mathbf{r}$ . We should emphasize that the localization function  $C_\sigma^{(q)}(\mathbf{r})$  is, in fact, a “delocalization” measure of the same kind of nucleons. The presence of the  $\alpha$  particle requires localization of nucleons with different spins and isospins, which cannot be quantified by  $C_\sigma^{(q)}(\mathbf{r})$ .

## III. NUMERICAL RESULTS

### A. Numerical details

In the present paper, instead of full Hartree-Fock-Bogoliubov (HFB) theory, we adopt the HF+BCS theory. It simplifies the numerical computation and allows us to examine the effect of the pairing in the local  $\alpha$ -removal strength. We truncate the model space for the pairing correlations. This is introduced by the number of

single-particle orbitals. For instance, for Sn isotopes, 82 neutron orbitals obtained in the HF+BCS are adopted for the neutron sector, while the protons are in the normal phase ( $\Delta_p = 0$ ) with 50 fully occupied orbitals. The neutron pairing gaps are determined by the third-order mass difference using the atomic mass evaluation [45, 46]:  $\Delta_n = 1.4, 1.2, 1.4$ , and  $1.3$  MeV for  $A = 112, 116, 120$ , and  $124$ , respectively.

We use the Skyrme energy density functional with the SkM\* parameter set [47]. We adopt the three-dimensional (3D) Cartesian grid representation of the square box, using the computer code developed in Refs. [48–50]. The 3D grid size is set to be  $(1.0 \text{ fm})^3$ . We adopt all the grid points inside a sphere of the radius of  $R = 12 \text{ fm}$ . The differentiation is evaluated with the nine-point finite difference. The center-of-mass correction is taken into account by modifying the nucleon’s mass as  $m \rightarrow m \times A/(A - 1)$ . The Coulomb potential is calculated by solving the Poisson equation with the conjugate-gradient method, in which the boundary values are constructed with the multipole expansion [51]. The single-particle orbitals are calculated with the imaginary-time method [52]. The iteration is carried out until the self-consistent solution is obtained.

### B. Even-even Sn isotopes

Since we neglect the rearrangement of the mean fields, the method is suitable for heavy nuclei in which the mean-field potentials are relatively stable against the removal of an  $\alpha$  particle (two protons and two neutrons). Since the ground states of Sn isotopes ( $Z = 50$ ) represent a typical example of pair-rotational bands in spherical nuclei [53], the mean fields should be stable with respect to the two-neutron removal. In contrast, the two-proton removal is expected to have a certain impact on the mean fields, because  $Z = 50$  is a spherical magic number for protons. Nonetheless, Cd isotopes ( $Z = 48$ ) exhibit typical excitation spectra of spherical vibrator [54]. Thus, it is meaningful to compare the magnitude of the local  $\alpha$ -removal strengths for different Sn isotopes ( ${}^A\text{Sn} \rightarrow {}^{A-4}\text{Cd}$ ).

#### 1. Normal density and pair density

First, let us show the density distributions for  ${}^{112,116,120,124}\text{Sn}$  in Fig. 2. The neutron radius increases as a function of the neutron number, while the proton radius stays almost constant. A dip in the central proton density can be understood as a shell effect because of the full occupation of the high- $j$  ( $g_{9/2}$ ) orbital. As we can expect, the neutron skin develops as increasing the neutron number. The neutron skin should have an impact on the  $\alpha$ -particle formation properties. Reference [37], using the Thomas-Fermi approximation, gave the  $\alpha$ -particle density in the surface region which decreases as the neutron

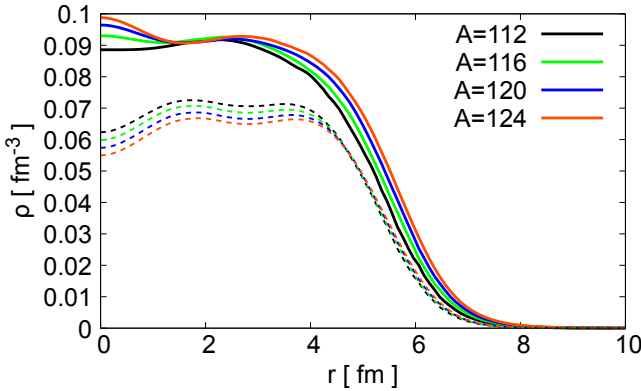


FIG. 2. Nucleon density distributions for neutrons (solid lines) and protons (dashed) for Sn isotopes ( $A = 112, 116, 120$ , and  $124$ ).

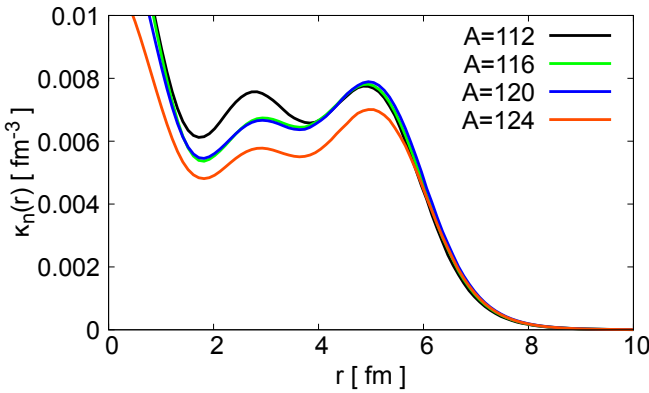


FIG. 3. Neutron pair density distributions for Sn isotopes ( $A = 112, 116, 120$ , and  $124$ ). The proton pair density vanishes for these isotopes.

skin increases. The  $\alpha$ -cluster formation is also predicted to have a negative impact on neutron skin thickness.

In Fig. 3, the neutron pair densities are shown. In the present calculation, the central peak at  $r \approx 0$  exists, which may be due to the monopole pairing interaction used in the BCS treatment and may depend on the type of pairing interaction. The surface peak is located at  $r \approx 5$  fm, whose shape is similar to each other. Since the proton number  $Z = 50$  is magic, the pair density vanishes for protons.

## 2. Local $\alpha$ -removal strengths

Since the numerical calculation is performed with the vanishing boundary condition, all the quasiparticle energies are discrete. To visualize the local  $\alpha$ -removal strength  $S_\alpha(r, E)$  as a function of excitation energy  $E$ , we replace the  $\delta$  function in Eq. (10) by the Gaussian function of the width of  $\gamma = 100$  keV. The calculated local  $\alpha$ -removal strengths for Sn isotopes are shown in Fig. 4.

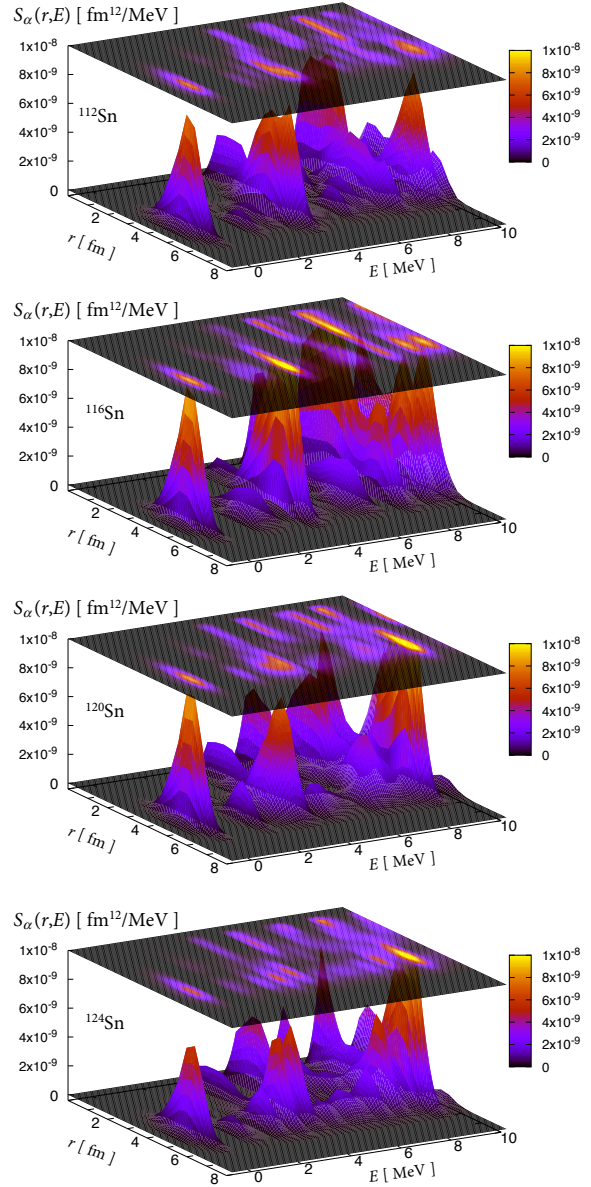


FIG. 4. Local  $\alpha$ -removal strengths  $S_\alpha(r, E)$  for Sn isotopes ( $A = 112, 116, 120$ , and  $124$ ). The energy  $E$  corresponds to the excitation energy of the residual nuclei after the removal of an  $\alpha$  particle at the radial position  $r$ . The discrete strengths are smeared by Gaussians with a width of 100 keV.

For each isotope, there is an isolated peak corresponding to the ground-ground transition ( $E = 0$ ). This  $\alpha$ -removal strength to the ground state is located near the surface region. At excitation energies of  $E \gtrsim 3$  MeV, there are peaks whose magnitude is comparable to or even larger than the transitions to the ground state. In contrast to the ground-ground transition, the strengths are not only in the surface region, but also in the interior region with  $r < 3$  fm. This indicates that the  $\alpha$  particle may exist deep inside the nucleus. However, in the  $\alpha$ -knockout reaction, these  $\alpha$  particles are difficult to come out of the

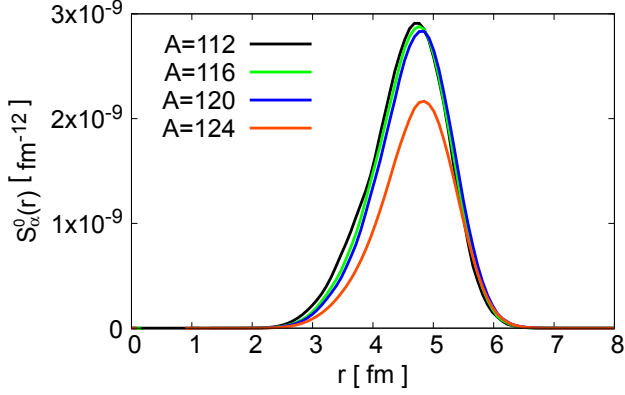


FIG. 5. Local  $\alpha$ -removal strength to the ground state  $S_\alpha^0(\mathbf{r})$  for Sn isotopes ( $A = 112, 116, 120$ , and  $124$ ).

nucleus because of the strong absorption. No strength is shown at  $r = 0$  in Fig. 4 that shows  $S_\alpha(\mathbf{r}, E)$  in the range of  $E < 10$  MeV. This is because the proton amplitude vanishes at  $r = 0$ ,  $F_k^{(p)}(0) = 0$ . The binding energy of the proton  $s_{1/2}$  state is larger than the  $g_{9/2}$  state, by more than 20 MeV. Thus, nonzero proton amplitude at the center  $F_k^{(p)}(0) \neq 0$  appears only for  $E > 40$  MeV.

### 3. Residual nuclei in the ground state

To examine the structure of the local  $\alpha$ -removal strengths to the ground state of the residual nuclei, in Fig. 5, we show the strength of Eq. (4) with  $E = 0$  and  $\Delta E \rightarrow 0+$ ,

$$\begin{aligned} S_\alpha^0(\mathbf{r}) &\equiv S_\alpha(\mathbf{r})_{E=0, \Delta E=2\epsilon} \\ &= \int_{-\epsilon}^{\epsilon} S_\alpha(\mathbf{r}, E) dE = F_0^{(n)}(\mathbf{r}) F_0^{(p)}(\mathbf{r}), \end{aligned} \quad (25)$$

where  $\epsilon$  is a positive infinitesimal. When we remove an  $\alpha$  particle at the position  $\mathbf{r}$ ,  $S_\alpha^0(\mathbf{r})$  can be regarded as a quantity proportional to the probability that the residual nucleus becomes the ground state. The shape of the peak is almost identical among these isotopes and located at  $r = |\mathbf{r}| \approx 4.7\text{--}4.8$  fm. This position approximately corresponds to the position  $r$  that gives  $\rho(\mathbf{r}) = (2/3) \times \rho(\mathbf{0})$  (Fig. 2). It is near the surface, however, the radial value  $r$  is significantly smaller than the peak position of the  $\alpha$  density  $n_\alpha(\mathbf{r})$  predicted in Ref. [37]. In fact, the peak position of the  $\alpha$  density  $n_\alpha(\mathbf{r})$  in Ref. [37] is located at  $6.5 < r < 7.5$  fm, which roughly corresponds to the value  $r$  with  $\rho_q(\mathbf{r}) \approx \rho_q(\mathbf{0})/10$ . The  $\alpha$  density  $n_\alpha(\mathbf{r})$  is predicted to vanish in the region of  $r < 6$  fm for Sn isotopes [37].

The peak height is similar to each other for  $^{112,116,120}\text{Sn}$ , while it is apparently smaller for  $^{124}\text{Sn}$ . This is naturally understood by the pair density in Fig. 3. The proton matrix elements  $F_0^{(p)}(\mathbf{r})$ , which is given by

Eq. (21), are determined by the HOO, namely  $g_{9/2}$  orbitals. They are surface peaked and approximately identical to each other among all the isotopes. The neutron matrix element  $F_0^{(n)}(\mathbf{r})$  is given by  $|\kappa_n(\mathbf{r})|^2$ , according to Eq. (14). Therefore, variations in  $S_\alpha^0(\mathbf{r}) = F_0^{(n)}(\mathbf{r}) F_0^{(p)}(\mathbf{r})$  come from those in  $F_0^{(n)}(\mathbf{r}) = |\kappa_n(\mathbf{r})|^2$ . A reduction in  $\kappa_n(\mathbf{r})$  at  $r \approx 5$  fm is the reason of the reduced peak height in  $S_\alpha^0(\mathbf{r})$  in  $^{124}\text{Sn}$ . This is easily confirmed by artificially increasing the neutron pairing gap: We have found that the peak height of  $S_\alpha^0(\mathbf{r})$  increases by about 50 % when we double the pairing gap  $\Delta_n$ .

The  $\alpha$ -knockout experimental data in Ref. [36] clearly indicate a monotonic decrease as a function of the neutron number. The experiment measures the missing-mass spectra to extract the cross section in which the residual nucleus is in the ground state. Therefore, this isotopic dependence should be related to  $S_\alpha^0(\mathbf{r})$  at the nuclear surface. The peak height of  $S_\alpha^0(\mathbf{r})$  shown in Fig. 5 is similar to each other except for  $^{124}\text{Sn}$ . Furthermore, they are almost identical at  $r \gtrsim 5.5$  fm where the  $\alpha$  knockout mainly takes place, namely,

$$S_\alpha^0(\mathbf{r})_{A=112} \approx S_\alpha^0(\mathbf{r})_{A=116} \approx S_\alpha^0(\mathbf{r})_{A=120} \approx S_\alpha^0(\mathbf{r})_{A=124}, \quad (26)$$

at  $r \gtrsim 5.5$  fm. In other words,  $S_\alpha^0(\mathbf{r})$  is universal for these isotopes in the surface region. This seems to be inconsistent with the experimental observation, at first sight.

However, we need to further examine the relationship between the cross section and the local  $\alpha$ -removal strength  $S_\alpha^0(\mathbf{r})$ . Since there is a strong absorption of the  $\alpha$  particle inside the nucleus, the cross section may not be correlated with the values at the same  $r$ , but we should compare those at a fixed value of nucleon density for each isotope. The nuclear radii apparently increase as the neutron number increases, because of the neutron skin effect (Fig. 2), namely  $R_{112} < R_{116} < R_{120} < R_{124}$ . Thus, the  $S_\alpha^0(\mathbf{r})$  values at the surface (fixed density) decrease as a function of the neutron number:

$$S_\alpha^0(\mathbf{R}_{112}) > S_\alpha^0(\mathbf{R}_{116}) > S_\alpha^0(\mathbf{R}_{120}) > S_\alpha^0(\mathbf{R}_{124}). \quad (27)$$

Therefore, the universal behavior of  $S_\alpha^0(\mathbf{r})$  may be consistent with the experimental observation.

To visualize this neutron number dependence, we define a dimensionless quantity, “local  $\alpha$  probability,” as the  $S_\alpha^0(\mathbf{r})$  value relative to the density.

$$P_\alpha^0(\mathbf{r}) \equiv \frac{S_\alpha^0(\mathbf{r})}{\rho_{n\uparrow}(\mathbf{r}) \rho_{n\downarrow}(\mathbf{r}) \rho_{p\uparrow}(\mathbf{r}) \rho_{p\downarrow}(\mathbf{r})}. \quad (28)$$

$P_\alpha^0(\mathbf{r})$  can be regarded as the probability to find an  $\alpha$  particle at the position  $\mathbf{r}$  under the condition that the residual nucleus is in the ground state, normalized to the probability of finding the four kinds of nucleons. The local  $\alpha$  probability is plotted in Fig. 6.  $P_\alpha^0(\mathbf{r})$  clearly indicates the monotonic decrease as the neutron number, which is consistent with the experiment [36].

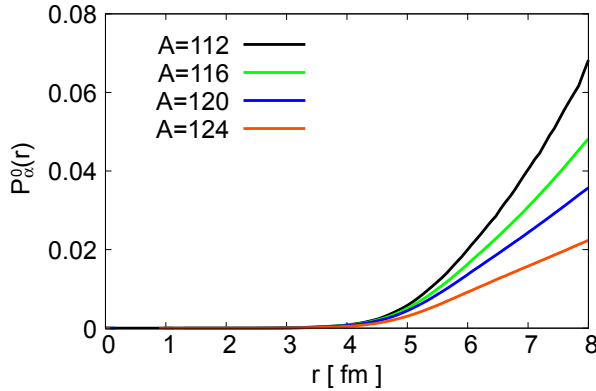


FIG. 6. Local  $\alpha$  probability  $P_\alpha^0(\mathbf{r})$  for Sn isotopes ( $A = 112, 116, 120$ , and  $124$ ).

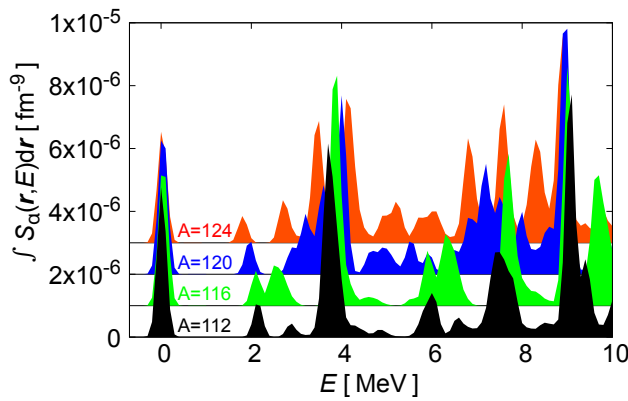


FIG. 7. Integrated local  $\alpha$ -removal strength  $\int S_\alpha(\mathbf{r}, E) d\mathbf{r}$  for Sn isotopes ( $A = 112, 116, 120$ , and  $124$ ). Those for  $A = 116, 120$ , and  $124$  are shifted upwards by  $10^{-6}$ ,  $2 \times 10^{-6}$ , and  $3 \times 10^{-6} \text{ fm}^{-9}$ , respectively.

#### 4. Excited residual nuclei

The local  $\alpha$ -removal strength, in principle, contains information on  $\alpha$  knockout to excited residual nuclei. Since the excited states are simply given by neutron 2qp states and proton particle-hole excitations, we should keep in mind that it is a qualitative measure. In Fig. 7,  $S_\alpha(\mathbf{r}, E)$  integrated over the space  $\mathbf{r}$  is shown for Sn isotopes. The small peak next to the ground state ( $E \approx 2$  MeV) corresponds to proton excitation in which one of the protons is removed from the  $g_{9/2}$  orbit and the other from  $p_{1/2}$ . The  $\alpha$ -removal strengths to some excited states of residual nuclei are as strong as those to the ground state.

It may be of interest to investigate the structure of the local  $\alpha$  probability when the residual nuclei are excited. Since there are two prominent peaks in Fig. 7, one around  $E \approx 4$  MeV and the other around 9 MeV, we set  $E = 4$  (9) MeV and  $\Delta E = 2$  MeV, to calculate the local  $\alpha$

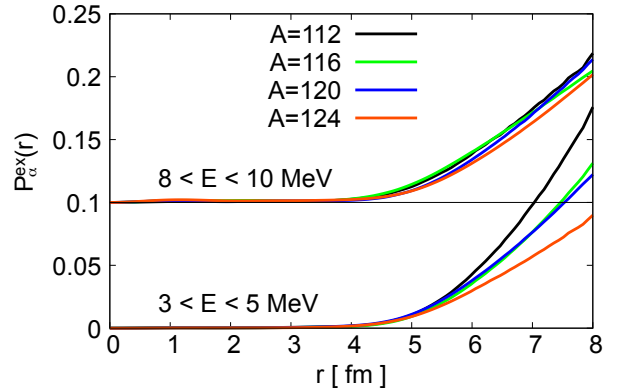


FIG. 8. Local  $\alpha$  probabilities for excited residual nuclei in Sn isotopes ( $A = 112, 116, 120$ , and  $124$ ), which are defined as Eq. (29) with  $E = 4$  MeV and  $\Delta E = 2$  MeV. Those with  $E = 9$  MeV are shifted upwards by 0.1.

probability as

$$P_\alpha^{\text{ex}}(\mathbf{r})_{E, \Delta E} \equiv \frac{\mathcal{S}_\alpha(\mathbf{r})_{E, \Delta E}}{\rho_{n\uparrow}(\mathbf{r})\rho_{n\downarrow}(\mathbf{r})\rho_{p\uparrow}(\mathbf{r})\rho_{p\downarrow}(\mathbf{r})}, \quad (29)$$

where  $\mathcal{S}_\alpha(\mathbf{r})_{E, \Delta E}$  is given by Eq. (4). These are shown in Fig. 8. The local  $\alpha$  probabilities for excited residual nuclei are enhanced in the low-density region. The monotonic increase as a function of  $r$  is the same as those to the ground state  $P_\alpha^0(\mathbf{r})$ , and seems to be universal. However, their isotopic dependence is not as prominent as  $P_\alpha^0(\mathbf{r})$ .  $P_\alpha^{\text{ex}}(\mathbf{r})_{E, \Delta E}$  with  $E = 9$  MeV and  $\Delta E = 2$  MeV for different isotopes are similar to each other. Since we neglect the effects of the rearrangement and the collective states, these numbers should not be taken seriously. Nevertheless, this may suggest that the  $\alpha$ -knockout reaction with excited residual nuclei may not show the prominent neutron number dependence, in contrast with those for the ground residual nuclei.

Integrating over the entire energy range, the total strength of the local  $\alpha$ -removal can be easily estimated in the mean-field approximation as

$$S_\alpha^{\text{tot}}(\mathbf{r}) = \int_{-\infty}^{\infty} S_\alpha(\mathbf{r}, E) dE = S_{\uparrow\downarrow}^{(n)}(\mathbf{r}) S_{\uparrow\downarrow}^{(p)}(\mathbf{r}), \quad (30)$$

where

$$\begin{aligned} S_{\uparrow\downarrow}^{(q)}(\mathbf{r}) &= \langle \Phi_0^{N_q} | \psi_{q\downarrow}^\dagger(\mathbf{r}) \psi_{q\uparrow}^\dagger(\mathbf{r}) \psi_{q\uparrow}(\mathbf{r}) \psi_{q\downarrow}(\mathbf{r}) | \Phi_0^{N_q} \rangle \\ &= \rho_{\uparrow}^{(q)}(\mathbf{r}) \rho_{\downarrow}^{(q)}(\mathbf{r}) - \left| \rho_{\uparrow\downarrow}^{(q)}(\mathbf{r}) \right|^2 + \left| \kappa^{(q)}(\mathbf{r}) \right|^2 \end{aligned} \quad (31)$$

The quantity of Eq. (30) can be written as  $S_\alpha^{\text{tot}}(\mathbf{r}) = \langle \Phi_0^A | \alpha^\dagger(\mathbf{r}) \alpha(\mathbf{r}) | \Phi_0^A \rangle$ , which may be regarded as the  $\alpha$ -particle density distribution. This is shown in Fig. 9. The major contribution to  $S_\alpha^{\text{tot}}(\mathbf{r})$  is the first term of Eq. (31), which is a local density product of nucleons with spin up and down. Thus,  $S_\alpha^{\text{tot}}(\mathbf{r})$  of Eq. (30) mainly comes from a trivial density product of four kinds of nucleons. This is nothing but the denominator of Eqs. (28)

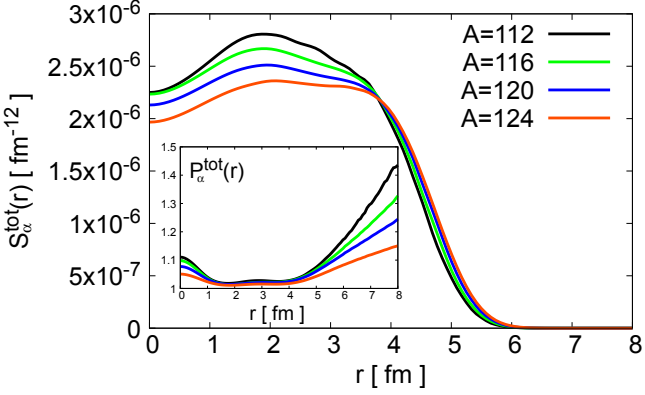


FIG. 9. Energy-integrated local  $\alpha$ -removal strength for Sn isotopes ( $A = 112, 116, 120$ , and  $124$ ).

and (29). If we normalize  $S_\alpha^{\text{tot}}(\mathbf{r})$  with respect to this trivial density product factor,

$$P_\alpha^{\text{tot}}(\mathbf{r}) \equiv \frac{S_\alpha^{\text{tot}}(\mathbf{r})}{\rho_{n\uparrow}(\mathbf{r})\rho_{n\downarrow}(\mathbf{r})\rho_{p\uparrow}(\mathbf{r})\rho_{p\downarrow}(\mathbf{r})}, \quad (32)$$

we obtain results shown in the inset of Fig. 9. Again, in the surface region, we observe the clear neutron-number dependence the same as  $P_\alpha^0(\mathbf{r})$  in Fig. 6.

If we neglect the second and the third terms in Eq. (31), we trivially have  $P_\alpha^{\text{tot}}(\mathbf{r}) = 1$ . Since the second term of Eq. (31) vanishes for the time-even ground state, the enhancement effect is due to the third term, namely, the effect of neutron pairing. Therefore, the surface  $\alpha$  formation may be understood as the fact that the pair density distribution is more extended than the normal density.

### 5. Localization function

Before closing this section, we examine the validity of the localization function. The calculated localization function  $C_\sigma(\mathbf{r})$  for Sn isotopes is presented in Fig. 10.  $C_\sigma(\mathbf{r})$  are approximately identical for all the isotopes. We observe a bump in  $C_\sigma(\mathbf{r})$  at  $r \approx 5$  fm for protons and at  $r \approx 5.5$  fm for neutrons. These values  $r$  of the peak positions are larger than those of  $S_\alpha^0(\mathbf{r})$  (Fig. 5). Besides, the profile of the function is significantly different between  $C_\sigma(\mathbf{r})$  and  $S_\alpha^0(\mathbf{r})$ . In comparison with the summed local  $\alpha$ -removal strength  $S_\alpha^{\text{tot}}(\mathbf{r})$  in Fig. 9, we again observe significantly different peak positions and profiles. There is no surface peak, and the peak structure almost disappears in Fig. 9. Therefore, it could be misleading to identify the localization function  $C_\sigma(\mathbf{r})$  as the indicator of the  $\alpha$ -particle formation in the mean-field theory.

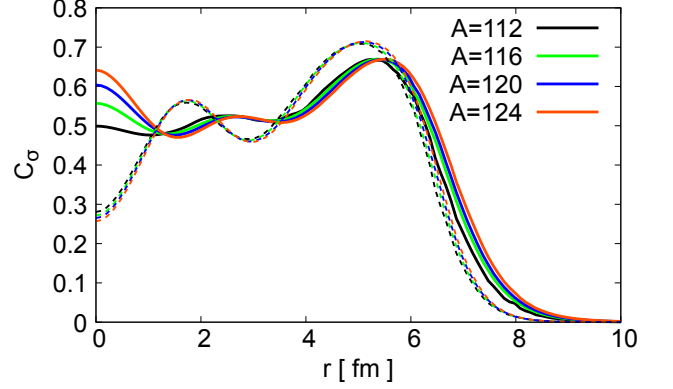


FIG. 10. Localization functions for neutrons (solid lines) and protons (dashed lines) for Sn isotopes ( $A = 112, 116, 120$ , and  $124$ ). The values with spin up ( $\sigma = +1/2$ )  $C_{+1/2}$  are shown in the figure, but those for spin down ( $\sigma = -1/2$ ) are identical.

## IV. CONCLUSION

To quantify the  $\alpha$ -particle formation, the local  $\alpha$ -removal strength  $S_\alpha(\mathbf{r}, E)$  is proposed. When we remove an  $\alpha$  particle at the position  $\mathbf{r}$  from a nucleus, the final state in the residual nucleus can be expanded in the energy eigenstates. The local  $\alpha$ -removal strength  $S_\alpha(\mathbf{r}, E)$  corresponds to the strength to produce the state at an energy  $E$  in the residual nucleus. This quantity is defined with respect to a many-body wave function, thus, it can be calculated using various quantum many-body techniques, in principle. The calculation becomes manageable when we adopt some approximations, such as the mean-field approximation (energy density-functional theory). Furthermore, if we neglect the rearrangement of the mean fields after the removal of an  $\alpha$  particle, the computational cost necessary for the local  $\alpha$ -removal strength is less than that for the mean-field calculation to obtain the ground state. We use these approximations in the present paper.

We calculate the local  $\alpha$ -removal strengths for Sn isotopes with  $A = 112, 116, 120$ , and  $124$ . These nuclei are studied by a recent  $\alpha$ -knockout experiment, in which the cross sections with the residual nuclei in the ground state clearly indicate a monotonically decreasing trend as a function of the neutron number. This prominent neutron-number dependence is not found in the  $\alpha$ -removal strength to the ground state,  $S_\alpha^0(\mathbf{r})$ , of Eq. (25). In fact, the function  $S_\alpha^0(\mathbf{r})$  is almost universal in the surface for all these isotopes. Nevertheless, the observed neutron-number dependence is well reproduced by the local  $\alpha$  probability,  $P_\alpha^0(\mathbf{r})$ , of Eq. (28). The monotonic decrease as a function of the neutron number is especially evident at the nuclear surface of  $r \gtrsim 6$  fm, where the  $\alpha$ -knockout reaction is supposed to take place.

It is also possible to explain the experimental trend using the universal character of  $S_\alpha^0(\mathbf{r})$  in the surface region

together with the development of the neutron skin. Since the absorption of the  $\alpha$  particle is strong, the knockout reaction is allowed only in the low-density region. This means that the radial value  $r$  of the region probed by the  $\alpha$ -knockout reaction is an increasing function of the neutron number. Therefore, the  $S_\alpha^0(\mathbf{r})$  values relevant to the knockout cross section decrease with the neutron number. This naturally explains the experimental data.

To identify the  $\alpha$  cluster, Ref. [33] proposed criteria combining the localization function with the compactness of the density localization. It may be useful for light deformed nuclei which show a prominent density localization. Apparently, the Sn isotopes in the present study satisfy none of these criteria; the ground states are spherical and show no density localization. On the other hand, the calculated local  $\alpha$ -removal strength to the ground state shows a surface peak structure and indicates the importance of the pair density. Since the pair density dominates over the normal density in the nuclear surface region, the last term of Eq. (31) should play a crucial role in the surface  $\alpha$  formation.

The local  $\alpha$ -removal strength in the present approximations can be calculated with a single state. In other words, the states in the residual nucleus are not constructed explicitly. Therefore, with a proper choice of the mean-field Hamiltonian, it can be evaluated in a time-dependent manner with the time-dependent density-functional theory (TDDFT). Recently, the nuclear TDDFT calculations have been renovated to include the pair density [49, 50, 55–59]. It is of significant interest to investigate the  $\alpha$ -particle formation probability during nuclear reactions, such as heavy-ion reactions,

fusion, and fission.

In the present paper, we introduce several approximations for feasibility of the numerical computation. The BCS approximation can be lifted and replaced by the full HFB calculation. It may be of interest to study how the type of the pairing interaction, such as volume or surface or mixed types, affects the  $\alpha$ -formation properties. We also neglect the rearrangement of the mean fields before and after the removal of an  $\alpha$  particle. The numerical calculation is extremely feasible with this approximation. However, it is a drastic approximation even for heavy nuclei. Especially, near the doubly closed nuclei, the nuclear shape may be changed, and the approximation may not be justified. To improve this, the calculation with proper treatment of the rearrangement is currently under progress. This may lead to a quantitative evaluation of the  $\alpha$ -knockout cross section. Furthermore, the inclusion of the proton-neutron pairing is an interesting subject in the future.

## ACKNOWLEDGMENTS

This work is supported in part by JSPS KAKENHI Grants No. JP18H01209, No. JP19H05142, No. JP23H01167, No. JP20K03964, and No. JP19KK0343. This research in part used computational resources provided by Multidisciplinary Cooperative Research Program in the Center for Computational Sciences, University of Tsukuba.

---

[1] K. Ikeda, N. Takigawa, and H. Horiuchi, *Prog. Theor. Phys. Suppl.* **E68**, 464 (1968).

[2] J. A. Wheeler, *Phys. Rev.* **52**, 1083 (1937).

[3] J. A. Wheeler, *Phys. Rev.* **52**, 1107 (1937).

[4] K. Ikeda *et al.*, *Prog. Theor. Phys. Suppl.* **68**, 1 (1980).

[5] M. Freer, H. Horiuchi, Y. Kanada-En'yo, D. Lee, and U.-G. Meißner, *Rev. Mod. Phys.* **90**, 035004 (2018).

[6] G. Gamow, *Z. Phys.* **51**, 204 (1928).

[7] G. Gamow and E. Rutherford, *Proc. R. Soc. London, Ser. A* **126**, 632 (1930).

[8] J. Chadwick, *Proc. R. Soc. London, Ser. A* **136**, 692 (1932).

[9] D. M. Brink, in *Many-Body Description of Nuclear Structure and Reactions: Proceedings of the International School of Physics “Enrico Fermi” Course XXXVI*, edited by C. Bloch (Academic Press, New York, 1966) pp. 247–276.

[10] H. Horiuchi, *Nucl. Phys. A* **522**, 257 (1991).

[11] H. Feldmeier, in *The Nuclear Equation of State: Part A: Discovery of Nuclear Shock Waves and the EOS*, edited by W. Greiner and H. Stöcker (Springer US, Boston, 1989) pp. 375–387.

[12] Y. Kanada-En'yo, M. Kimura, and A. Ono, *Prog. Theor. Exp. Phys.* **2012**, 01A202 (2012).

[13] H. Feldmeier and J. Schnack, *Prog. Part. Nucl. Phys.* **39**, 393 (1997).

[14] H. Feldmeier and J. Schnack, *Rev. Mod. Phys.* **72**, 655 (2000).

[15] D. L. Hill and J. A. Wheeler, *Phys. Rev.* **89**, 1102 (1953).

[16] J. J. Griffin and J. A. Wheeler, *Phys. Rev.* **108**, 311 (1957).

[17] S. Takami, K. Yabana, and K. Ikeda, *Prog. Theor. Phys.* **96**, 407 (1996).

[18] H. Ohta, K. Yabana, and T. Nakatsukasa, *Phys. Rev. C* **70**, 014301 (2004).

[19] J. A. Maruhn, M. Kimura, S. Schramm, P.-G. Reinhard, H. Horiuchi, and A. Tohsaki, *Phys. Rev. C* **74**, 044311 (2006).

[20] J. A. Maruhn, N. Loebel, N. Itagaki, and M. Kimura, *Nucl. Phys. A* **833**, 1 (2010).

[21] Y. Fukuoka, S. Shinohara, Y. Funaki, T. Nakatsukasa, and K. Yabana, *Phys. Rev. C* **88**, 014321 (2013).

[22] J.-P. Ebran, E. Khan, T. Nikšić, and D. Vretenar, *J. Phys. G* **44**, 103001 (2017).

[23] J.-P. Ebran, E. Khan, T. Nikšić, and D. Vretenar, *Nature* **487**, 341 (2012).

[24] M. Matsumoto and Y. Tanimura, *Phys. Rev. C* **106**, 014307 (2022).

[25] P.-G. Reinhard, J. A. Maruhn, A. S. Umar, and V. E. Oberacker, *Phys. Rev. C* **83**, 034312 (2011).

[26] A. D. Becke and K. E. Edgecombe, *J. Chem. Phys.* **92**, 5397 (1990).

[27] C. L. Zhang, B. Schuetrumpf, and W. Nazarewicz, *Phys. Rev. C* **94**, 064323 (2016).

[28] B. Schuetrumpf and W. Nazarewicz, *Phys. Rev. C* **96**, 064608 (2017).

[29] T. Inakura and S. Mizutori, *Phys. Rev. C* **98**, 044312 (2018).

[30] Y. Tanimura, *Phys. Rev. C* **99**, 034324 (2019).

[31] F. Mercier, A. Bjelčić, T. Nikšić, J.-P. Ebran, E. Khan, and D. Vretenar, *Phys. Rev. C* **103**, 024303 (2021).

[32] Z. X. Ren, D. Vretenar, T. Nikšić, P. W. Zhao, J. Zhao, and J. Meng, *Phys. Rev. Lett.* **128**, 172501 (2022).

[33] E. Khan, L. Heitz, F. Mercier, and J.-P. Ebran, *Phys. Rev. C* **106**, 064330 (2022).

[34] T. A. Carey, P. G. Roos, N. S. Chant, A. Nadasen, and H. L. Chen, *Phys. Rev. C* **23**, 576 (1981).

[35] P. G. Roos, N. S. Chant, A. A. Cowley, D. A. Goldberg, H. D. Holmgren, and R. Woody, III, *Phys. Rev. C* **15**, 69 (1977).

[36] J. Tanaka, Z. Yang, S. Typel, S. Adachi, S. Bai, P. van Beek, D. Beaumel, Y. Fujikawa, J. Han, S. Heil, S. Huang, A. Inoue, Y. Jiang, M. Knösel, N. Kobayashi, Y. Kubota, W. Liu, J. Lou, Y. Maeda, Y. Matsuda, K. Miki, S. Nakamura, K. Ogata, V. Panin, H. Scheit, F. Schindler, P. Schrock, D. Symochko, A. Tamii, T. Uesaka, V. Wagner, K. Yoshida, J. Zenihiro, and T. Aumann, *Science* **371**, 260 (2021).

[37] S. Typel, *Phys. Rev. C* **89**, 064321 (2014).

[38] K. Yoshida, K. Minomo, and K. Ogata, *Phys. Rev. C* **94**, 044604 (2016).

[39] B. Brémond and J. G. Valatin, *Nucl. Phys.* **41**, 640 (1963).

[40] A. L. Goodman, *Nucl. Phys. A* **186**, 475 (1972).

[41] E. Perlińska, S. G. Rohoziński, J. Dobaczewski, and W. Nazarewicz, *Phys. Rev. C* **69**, 014316 (2004).

[42] K. Sato, J. Dobaczewski, T. Nakatsukasa, and W. Satuła, *Phys. Rev. C* **88**, 061301 (2013).

[43] J. A. Sheikh, N. Hinohara, J. Dobaczewski, T. Nakatsukasa, W. Nazarewicz, and K. Sato, *Phys. Rev. C* **89**, 054317 (2014).

[44] P. Ring and P. Schuck, *The Nuclear Many-Body Problems*, Texts and monographs in physics (Springer-Verlag, New York, 1980).

[45] W. J. Huang, M. Wang, F. G. Kondev, G. Audi, and S. Naimi, *Chin. Phys. C* **45**, 030002 (2021).

[46] M. Wang, W. J. Huang, F. G. Kondev, G. Audi, and S. Naimi, *Chin. Phys. C* **45**, 030003 (2021).

[47] J. Bartel, P. Quentin, M. Brack, C. Guet, and H.-B. Häkansson, *Nucl. Phys. A* **386**, 79 (1982).

[48] T. Nakatsukasa and K. Yabana, *Phys. Rev. C* **71**, 024301 (2005).

[49] S. Ebata, T. Nakatsukasa, T. Inakura, K. Yoshida, Y. Hashimoto, and K. Yabana, *Phys. Rev. C* **82**, 034306 (2010).

[50] S. Ebata, T. Nakatsukasa, and T. Inakura, *Phys. Rev. C* **90**, 024303 (2014).

[51] H. Flocard, S. E. Koonin, and M. S. Weiss, *Phys. Rev. C* **17**, 1682 (1978).

[52] K. T. R. Davies, H. Flocard, S. Krieger, and M. S. Weiss, *Nucl. Phys. A* **342**, 111 (1980).

[53] D. M. Brink and R. A. Broglia, *Nuclear Superfluidity, Pairing in Finite Systems* (Cambridge University Press, Cambridge, 2005).

[54] A. Bohr and B. R. Mottelson, *Nuclear Structure, Vol. II* (W. A. Benjamin, New York, 1975).

[55] B. Avez, C. Simenel, and P. Chomaz, *Phys. Rev. C* **78**, 044318 (2008).

[56] I. Stetcu, A. Bulgac, P. Magierski, and K. J. Roche, *Phys. Rev. C* **84**, 051309 (2011).

[57] Y. Hashimoto, *Eur. Phys. J. A* **48**, 55 (2012).

[58] Y. Hashimoto and G. Scamps, *Phys. Rev. C* **94**, 014610 (2016).

[59] P. Magierski, K. Sekizawa, and G. Włazłowski, *Phys. Rev. Lett.* **119**, 042501 (2017).